View metadata, citation and similar papers at core.ac.uk

brought to you by CORE

provided by NASA Technical Reports Server

TECHNICAL REPORT STANDARD TITLE PAGE

1. Report No.	2. Government Accession No.	3. Recipient's Catalog No.
4. Title and Subtitle "SYSTEM IMPLICATIONS OF LARGE RADIOMETRIC ARRAY ANTENNAS"		5. Report Date June 1976 6. Performing Organization Code
7. Author(s) C. A. Levis & H. C. Lin		8. Performing Organization Report No. ESL 3931-2
9. Performing Organization Name and Address The Ohio State University ElectroScience Laboratory, Department of Electrical Engineering, Columbus, Ohio 43212		10. Work Unit No. 11. Contract or Grant No. NAS5-20521
12. Sponsoring Agency Name and Address National Aeronautics and Space Administration Goddard Space Flight Center, Greenbelt MD E. Hirschmann, Code 951, Technical Officer		13. Type of Report and Period Covered Type II 5/16/74 to 9/30/75 14. Sponsoring Agency Code

15. Supplementary Notes

16. Abstract

Current radiometric earth and atmospheric sensing systems in the centimeter wavelength range generally employ a directive antenna connected through a single terminal pair to a Dicke receiver. It is shown that this approach does not lend itself to systems with greatly increased spatial resolution. Signal-to-noise considerations relating to antenna efficiency force the introduction of active elements at the subarray level; thus, if Dicke switching is to be used, it must be distributed throughout the system. Some possible approaches are suggested. The introduction of active elements at the subarray level is found to ease the design constraints on time delay elements, necessary for bandwidth, and on multiple-beam generation, required in order to achieve sufficient integration time with high resolution.

17. Key Words (Selected by Author(s))		18. Distribution Statement
antenna	radiometer	
array	resolution	
efficiency	remote sensing	

19. Security Classif. (of this report)	20. Security Classif. (of this page)	21. No. of Pages	22. Price*
U	U	21	

*For sale by the Clearinghouse for Federal Scientific and Technical Information, Springfield, Virginia 22151.

PREFACE

The objective of this contract is to define feasible and useful experiments employing a large millimeter-wave electronically steerable antenna on vehicles of the Space Shuttle generation. The large weight and size capability of such vehicles potentially allows antenna systems to be employed which exceed those of current aircraft and satellite systems by an order of magnitude in linear dimension. This report is concerned specifically with the implication of such a large antenna on a radiometric earth-sensing system for which it is to be the signal source.

The chief advantage of a large antenna to a radiometric system is its potential for increased spatial resolution. In this report it is shown that this potential cannot be realized with conventional systems because of the effect of antenna losses. Some possible approaches for realizing the inherent resolution potential of large antennas are suggested.

CONTENTS

I. INTRODUCTION

Imaging microwave radiometers are being used increasingly to sense remotely geophysical parameters such as sea state, sea ice distribution, cloud types and distributions, and soil moisture. Instruments of this type which have evolved over the past decade differ considerably in details of design; nevertheless two basic performance parameters, viz., their angular or spatial resolution and their temperature resolution or sensitivity, have remained relatively constant over this period. This is illustrated in Table I, which compares four such systems in the range of 15 to 40 GHz [1-4]. The angular resolutions of these systems are determined primarily by the size of their antennas, which is on the order of one meter in linear dimension for each. That size was determined principally by considerations of the maximum size and weight allowable for the respective vehicles, aircraft in the case of the AN/AAR-33 and satellites for the others.

The capabilities of the Space Shuttle will greatly exceed the allowable weights and dimensions of earlier satellite payloads [5]. An antenna approximately 10 meters by 10 meters in size and operable in the 10-100 GHz region was proposed in the initial experiment definition stage of a Space Shuttle experiment [6,7]. In principle, an aperture of this size should allow an increase in angular resolution (decrease in beamwidth) by an order of magnitude. Even larger antennas are envisioned in space at a later date [8]. The question addressed here is to what extent such antennas will be compatible with the remainder of radiometric imaging systems as they are now implemented on aircraft and satellites. It will be found that major changes in system design are required. These changes are dictated by considerations of integration time, bandwidth, and antenna losses. Of these, the antenna losses seem to have received the least attention so far, and yet they have the most far-reaching implications. Moreover, it turns out that proposed solutions for the antenna - loss problem also increase the degrees of freedom for solving the others.

II. BASIC CONSIDERATIONS

A. General

To our best knowledge, all current and proposed aircraft and satellite imaging radiometers are of the Dicke-switch type [9], shown in simplified form in Fig. 1. The receiver input is switched at an audio rate between the antenna and a comparison load which is kept at a known temperature T_1. The switching modulates the noise signal at the audio rate; it is then amplified. Several frequency translations may take place in this process; finally, it is detected synchronously with respect to the switch modulation, integrated, and recorded. At less frequent intervals, another load at a known temperature T_2, different from T_1, is substituted for T_1. The difference in response can be used to calibrate the receiver gain or, as indicated in the figure, to stabilize it via a feedback loop. The limitations which arise with such a system can best be understood by referring to the basic equation for the sensitivity or temperature resolution of such a device [10,11],

$$\Delta T = \frac{k_1 T_{in}}{\sqrt{B\tau}} \cdot S' \qquad (1)$$

In this equation, ΔT denotes the minimum detectable change of temperature at the receiver input, k_1 is a constant (typically about 2) depending on the modulation waveform of the switching and the bandwidth of the post-detection filtering, B is the pre-detection bandwidth, and τ is the time available for integration. When a simple low-pass filter is used for the integration, τ can be replaced by ω_L^{-1}, the reciprocal of the angular cut-off frequency of the integrating filter [12]. S' is a system stability factor; the purpose of the second comparison load is to maintain S' near unity. The system input temperature is given by

$$T_{in} = 290(F-1) + T_{ant} \qquad (^{o}K) \qquad (2)$$

where F is the standard receiver noise figure and T_{ant} the effective antenna temperature, given by [13,14]

$$T_{ant} = \eta \int T_b(\Omega)\, f(\Omega)\, d\Omega + (1-\eta)\, T_p \qquad (3)$$

where η is the combined power efficiency of the antenna and the network connecting it to the receiver, $f(\Omega)$ is the antenna power pattern normalized so that its integral over all directions Ω is unity, T_b is the brightness temperature distribution observed by the antenna, and T_p is the physical temperature of the antenna and feed system.

B. Integration Time

If the spatial resolution of the array is to be maximized, the integration time in equation (1) must be chosen commensurate with the spatial resolution of the antenna; i.e., τ should not be larger than the time during which the combination of scanning and vehicle motion displaces the antenna beam by one beamwidth. This requirement prevents adjacent resolution elements from becoming blurred by the integration process. On the other hand, equation (1) shows that τ should be as large as possible, consistent with the preceding limitation, in order to minimize ΔT and thus maximize sensitivity. The integration-time dilemma is now obvious. If the antenna beamwidth is divided by n in each plane, for an aircraft or low-orbit satellite system this will require a multiplication of the transverse scan rate by n; also n times as many resolution cells will need to be accommodated within each scan (assuming constant swath width). Thus the integration time available per resolution element will be decreased by a factor of n^2, increasing the temperature uncertainty ΔT by a factor of n according to equation (1). A possible way to circumvent this problem would be the use of multiple beams as indicated in Fig. 2. This approach does not turn out to be useful, however, because of the losses introduced by the beam-forming network. As will be shown below, the large array antenna is in quite sufficient trouble because of basic antenna losses without the addition of any further network losses between the elements and the Dicke-switch.

C. Array Bandwidth

The frequency bandwidth of antenna arrays is well known to be inversely proportional to the maximum array dimension when the phase shifter characteristics are assumed to produce a phase shift which is independent of frequency. Thus an increase in antenna size would decrease the pre-detection bandwidth B and, according to equation (1), affect sensitivity adversely. This effect can be overcome by the use of true time delays instead of phase shifters, or, what is equivalent, of phase shifters whose phase shift at any phase shift setting is directly proportional to frequency over the bandwidth of the radiometer. Such devices are, however, not readily availble in the centimeter wavelength range, especially if the requirements of good phase stability and low loss are added.

D. Antenna Losses

The effect of antenna losses seems to have received relatively less attention in the literature, yet it becomes of great importance as antenna size is increased. Before dealing with this concept quantitatively, a brief intuitive discussion may be in order. In present array technology, the elements are connected to the Dicke-switch via a network of transmission lines (generally waveguides), power dividers, and phase shifters. As the array size is increased, the transmission line lengths increase and so does the number of power dividers, hence the efficiency decreases. If the array is looking at a constant brightness temperature T_b, the integral in equation (3) is independent of antenna pattern and becomes

$$T_{ant} = \eta T_b + (1-\eta)T_p \quad . \tag{4}$$

Since the first term represents the radiometric signal while the second represents internal noise, we can define a radiometric signal-to-noise ratio

$$S/N = \eta T_b/(1-\eta)T_p \tag{5}$$

and a relative (temperature-independent) ratio

$$R' \equiv (S/N)/(T_b/T_p) = \eta/(1-\eta) \quad . \tag{6}$$

From this relationship it is apparent that an increase in array size, with its accompanying decrease in efficiency, lowers the radiometric signal-to-noise ratio.

Another intuitive way of looking at the problem is to consider first a small array and then the large array that can be derived from it by the addition of more elements, as in Fig. 3. The added elements, having longer transmission paths, contribute less signal and more thermal noise relative to those of the small array. Thus, assuming the aperture illumination taper is not changed, the large array will have better spatial resolution but poorer sensitivity than the smaller.

III. RELATIVE SIGNAL-TO-NOISE RATIO CALCULATIONS

These intuitive concepts will now be put on a firmer, numerical basis. Calculations have been made for a variety of feed configurations; here we will use as an example the case of a uniformly corporate-fed antenna, with the elements arranged in groups of four at each level. The element geometry is a square grid as shown in Fig. 4. To illustrate the method of connection, the one-dimensional analog is shown in Fig. 5 in which elements are connected repeatedly in groups of two. The two-dimensional analog is not easy to show on paper because the transmission line paths overlap, but the scheme is indicated in Fig. 6. Four adjacent elements are first combined into first stages (analogous to groupings of two elements in the one-dimensional case); four first-stage groups, consisting of 4 elements each, are combined into second-stage groups (analogous to the four-element groupings in the one-dimensional array), etc. By examining the behavior of the array as the number of stages increases, a wide range of array sizes can be examined. The number of elements is 4^r, where r is the number of stages or levels of combining.

First let us examine the signal-to-noise ratio as a function of array size when the array is used as a receiver for point-source radiation as in a communications receiver. Since the antenna is a linear device, the signal received will always be proportional to the field strength. Thus if we denote by S_0 the signal available at each element (in the presence of all other elements, i.e., with coupling effects taken into account but neglecting edge effects since the array is large) then the signal delivered to the final summation point will be proportional to S_0. On the other hand, the noise contributions due to losses in the antenna system will be proportional to kT_pB, where k is Boltzman's constant and T_p and B are the physical antenna temperature and rf bandwidth, as before. Since these quantitites are not directly related to properties of the antenna, the calculations which follow deal with normalized signals s, (the actual signal divided by S_0) and normalized noise n, (the actual noise power divided by kT_pB). This yields a normalized signal-to-noise ratio R

$$R = s/n \quad , \tag{7}$$

from which the actual signal-to-noise ratio may be computed by

$$S/N = R(S_0/kT_pB) \quad . \tag{8}$$

The normalized signal can be computed for a r-level corporate-fed network by a recursive process [15]

(9) $$s_1 = 4Te^{-2\alpha d_1}, \quad d_1 = d/\sqrt{2},$$

(10) $$s_q = 4s_{q-1}e^{-2\alpha d_q}, \quad d_q = 2d_{q-1}, \quad q = 2, \cdots, r,$$

and the normalized noise can similarly computed as

(11) $$n_1 = 1-Te^{-2\alpha d_1}$$

(12) $$n_q = 1+(n_{q-1}-1)e^{-2\alpha d_q}, \quad q = 2, \cdots, r,$$

where α is the logarithmic attenuation coefficient of the transmission lines (nepers per unit length) and T is the power transmission coefficient of the phase shifters. Loss in the power combiners has been ignored, thus producing a deliberately optimistic estimate of the normalized signal-to-noise ratio. The inclusion of loss in the power dividers is not unduly complicated [16,17], but it merely introduces an additional parameter which has the same effect as increasing the transmission line attenuation. A plot of the normalized signal-to-noise ratio of the square corporate-fed array discussed above, operating at 30 GHz, is shown in Fig. 7. Numerous curves for other element spacings, loss parameters, and feed configurations may be found in reference [15], which also lists the computer (Fortran IV) codes for their generation. All show the same characteristic shape: at a characteristic size, typically approximately 10 meters on a side at 30 GHz, the signal-to-noise ratio begins to saturate and then decreases.

The preceding calculation considered the case of a spatially coherent signal, i.e., one arriving from a specific direction, as in a communications situation. In the radiometric application, the radiometric signal arrives over a range of directions, and the output temperature of the antenna is given by equation (3) as the convolution of the normalized antenna power pattern with the spatial brightness distribution seen by the antenna. A different output will, of course, be obtained for different brightness distributions; we shall assume here that the brightness is constant over the largest resolution element, i.e. the greatest antenna beamwidth to be considered. It would, of course, be possible to calculate the efficiency of each array configuration and obtain the signal-to-noise ratio by equation (6). An alternate method was used which yields the same result. It is based on the observation that for the corporate-fed arrays examined here, the beamwidth varies inversely as the linear dimension since the aperture distribution remains unchanged as elements are added by increasing the number of stages. Thus the beam area varies inversely as the number of elements, m, where m is related to the number of stages or feed levels r by

(13) $$m = 4^r \quad .$$

Since contributions to the radiometric antenna temperature add in coherent fashion only from directions within the beamwidth of the antenna, the radiometric signal decreases as 1/m, while the thermal noise contribution remains that as given by equation (12). As a result, a value of the relative signal-to-noise performance of the array for radiometric application can be obtained by simply dividing each value of R in Fig. 7 by the number of elements in the array, m. The result is shown in Fig. 8; it is consistent with equation (6).

It is evident in this figure that for small numbers of elements the radiometric signal-to-noise ratio is independent of the number of elements and therefore of the beamwidth. This well-known behavior is also evident from equation (6). For small arrays, the transmission line losses are small compared to those in the phase shifters, and the efficiency is relatively constant until the increased size makes the transmission line losses comparable to the phase shifter losses. Beyond this point, the radiometric signal-to-noise ratio deterioriates dramatically, and it can be seen that for 30 GHz the one-meter dimension of current radiometric arrays is near the knee of the curve. Since the Nimbus arrays are not corporate-fed structures, no precise conclusions should be drawn from this fact; yet it is suggestive of the possibility that scaling of such systems by an order of magnitude would run into serious difficulties from the standpoint of radiometric signal-to-noise ratio. This is further supported by equation (3) and the fact that the antenna loss for the Nimbus F radiometer is on the order of 2.8 dB, corresponding to an efficiency of about 52% [4].

The corporate-fed structure with uniform distribution, which has been discussed so far, is unique in preserving the same transmission-line length between all elements and the feed-point; both the signal and the noise from each element contribute therefore to the sum signal with equal weight, compared to any other element. This is not true of other configurations. The examination of at least one other configuration is instructive because it illustrates the tradeoffs between signal-to-noise performance (and therefore sensitivity) and angular resolution which are possible. Consider a centrally parallel-fed square array. The geometry is precisely as shown in Fig. 4. Each element is connected to the feedpoint via the shortest possible transmission path and a single phase shifter; at the feed all signals are combined in a single lossless combiner. (Such a device does not exist, but it is possible in principle and convenient for the illustration.) Suppose the designer has the choice of combining the signals from the elements with arbitrary weights. If he chooses to utilize a uniform aperture distribution, he

has to assign the highest weights to the furthest elements because these have the highest transmission losses; in fact, the weights will have to be precisely inversely proportional to the transmission loss from each element. The pattern will then be that of a uniform amplitude distribution, with the corresponding good resolution, but the signal-to-noise ratio will suffer because the signals with most strongly attenuated signal and greatest thermal noise at the summing point will be emphasized. Alternatively, the designer may choose to combine the signals in an optimum S/N ratio combiner sense, i.e., with weights proportional to the signal-to-noise ratio of each input at the summing point. This would emphasize the near-in elements and greatly de-emphasize the far elements; consequently the resolution gain due to the far elements becomes marginal for large arrays. It is seen that the signal-to-noise ratio vs. resolution dilemma is not limited to the corporate-fed array discussed above but is a general feature of large arrays. The uniformly weighted parallel array is discussed in more detail in reference [15], and computer codes for the calculations are given there.

IV. POSSIBLE SOLUTIONS

From the preceding discussion it is apparent that it is not satisfactory to allow a long lossy transmission path between distant array elements and the final summing point. One method of avoiding this is to divide the array into subarrays and to introduce amplification at the subarray level. This means, however, that if Dicke-switching is to be used then it must also occur at the subarray level. One possible general configuration of such a system is shown in Fig. 9. The switches are all synchronized, so that all subarrays are connected to their respective switches simultaneously. Since the signals following amplification are at a high level, the signal-to-noise ratio is established at this point and losses further down the signal path have little effect. It becomes therefore possible to convert the signal to other frequencies; for example f_2 could be chosen so as to optimize the linearity of the time delays (which could be quite lossy, e.g., acoustical devices might be used); and f_3 could be chosen to optimize the beam-forming matrix, which also could be lossy in this system. In this way the introduction of distributed Dicke-switching and amplification at the subarray level would help not only in regard to maintaining radiometric signal-to-noise ratio but it would also ease the design problems associated with bandwidth and integration time (by use of multiple beams) by allowing the use of lossy devices in optimized intermediate-frequency ranges. There are of course numerous engineering problems to be resolved, e.g., the synchronization and distribution of the local oscillator signals over the structure. In truly large arrays this might be accomplished by phase-locking local sources to a master oscillator by means of modulated optical signals transmitted to the subarrays. We do not pretend to have reduced such a system to practice; we are merely suggesting it as one possible means of avoiding the basic problems which arise when the present two-terminal antenna/single Dicke-switch system is extended to much larger apertures.

Other approaches are worthy of exploration. Among these are correlation arrays [12] which are finding increasing application in radio astronomy [18,19]. They require extensive data processing, but in consideration of the weight capabilities of such vehicles as the Space Shuttle and the advent of microprocessors they should not be ruled out. Most applications of such arrays in astronomy have led to their evaluation for the mapping of point sources or sources of limited extent surrounded by much larger cold regions. Their consideration for earthward sensing would seem to deserve more consideration.

V. CONCLUSIONS

The extension of present remote-sensing radiometry techniques to larger systems for higher spatial resolution is hindered primarily by antenna-loss effects which reduce temperature sensitivity. Bandwidth and integration time are also considerations which complicate the use of large antennas. The introduction of active devices at the subarray level, with consequent system modifications such as distributed Dicke-switching or correlation detection, appear to merit further development if orders-of-magnitude increases in resolution are to be realized.

RADIOMETER CHARACTERISTICS

	AN/AAR-33	Sea Sat-A	Nimbus E	Nimbus F
Date	1967	Proposed	1972	1975
Frequency (GHz)	15	18,22,36	19.35	37
Antenna	Paraboloids	Paraboloids	Array	Array
Beamwidth	2.2° x 1.7°	1.5° x 1.5° to 0.74° x 0.74°	1.4° x 1.4°	1.2° x 0.7°
ΔT(°K)	1.7	0.6 - 0.9	1.5	1

Table I

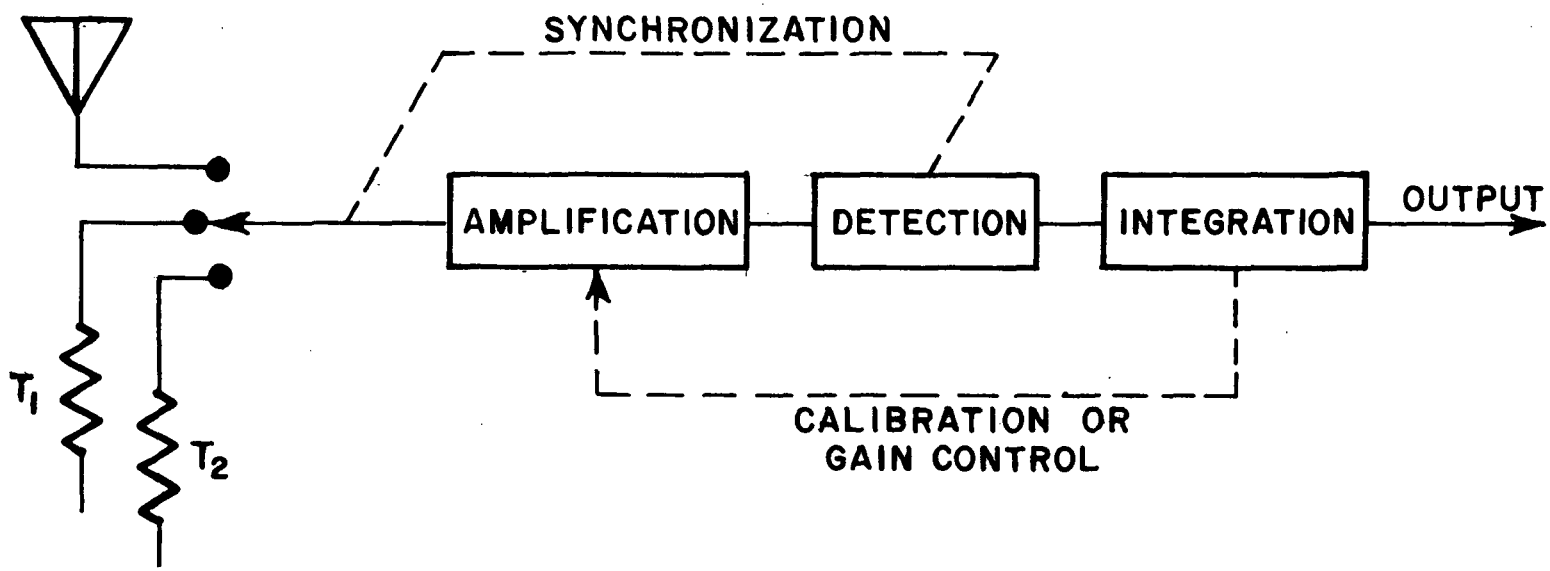

Figure 1. Calibrated Dicke radiometric receiver

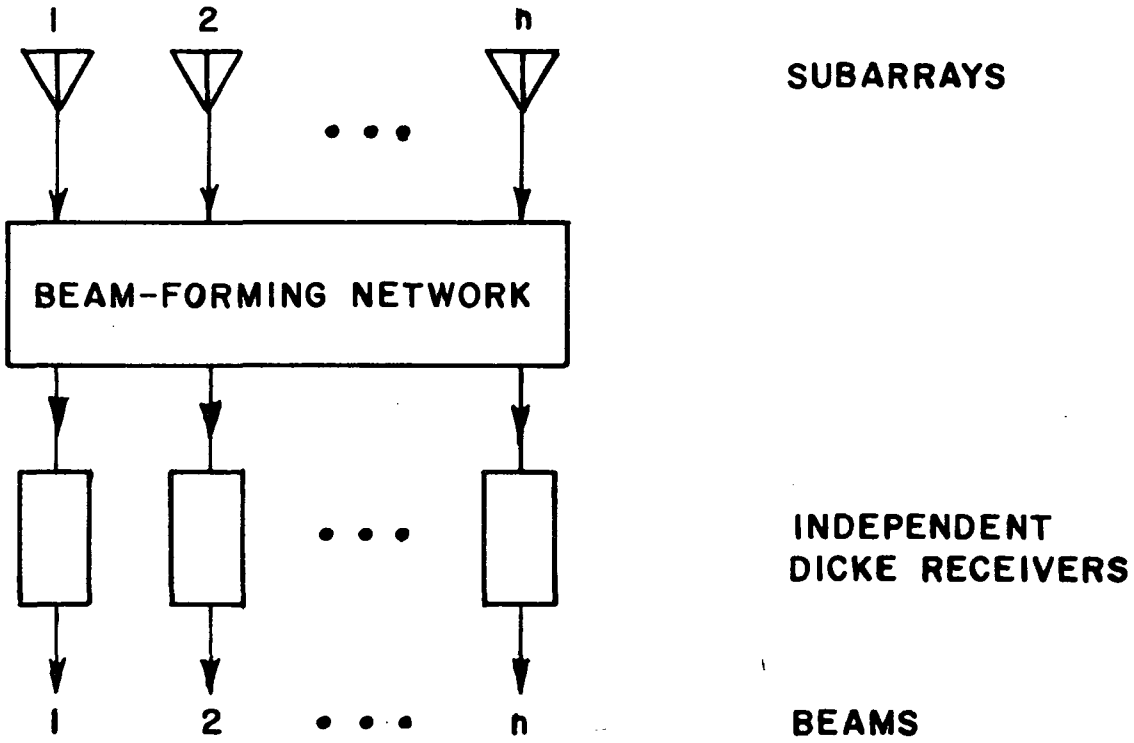

Figure 2. Multiple-beam radiometer with radio-frequency beam-forming

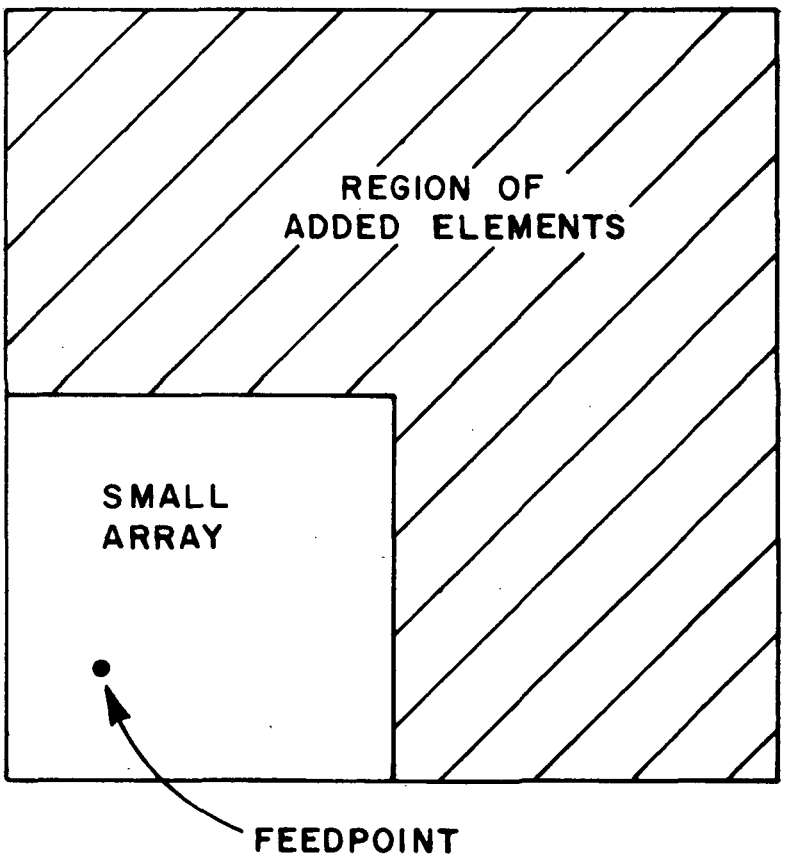

Figure 3. Large array, considered as a smaller array with added elements

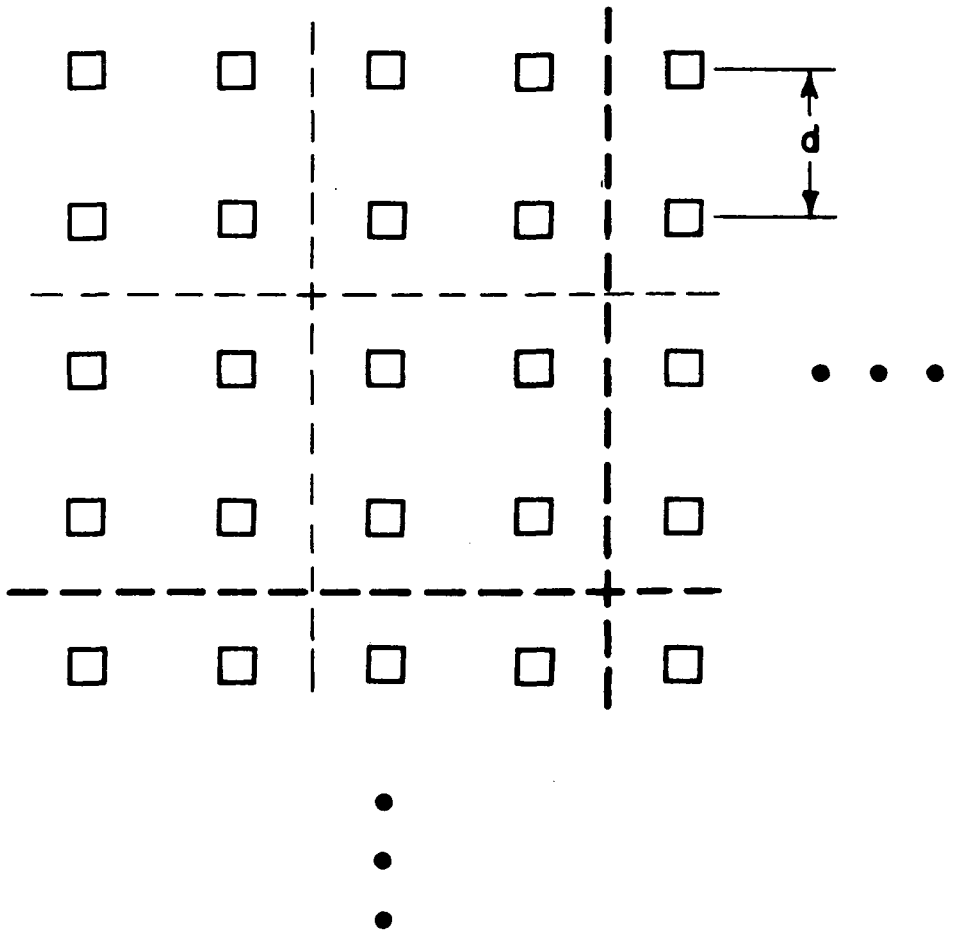

Figure 4. Array geometry for two-dimensional corporate-fed antenna

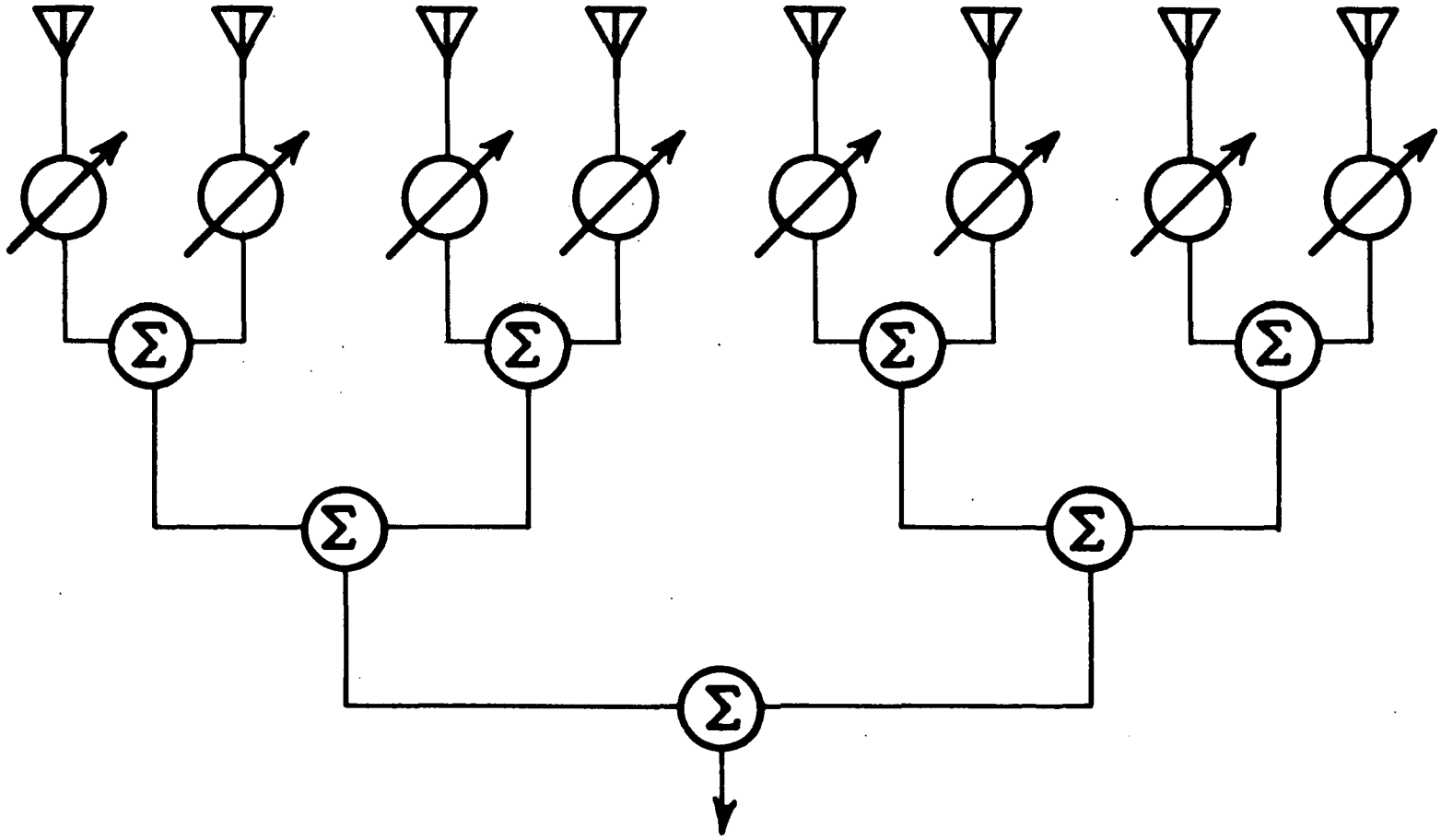

Figure 5. One-dimensional analog for the two-dimensional corporate-fed array.

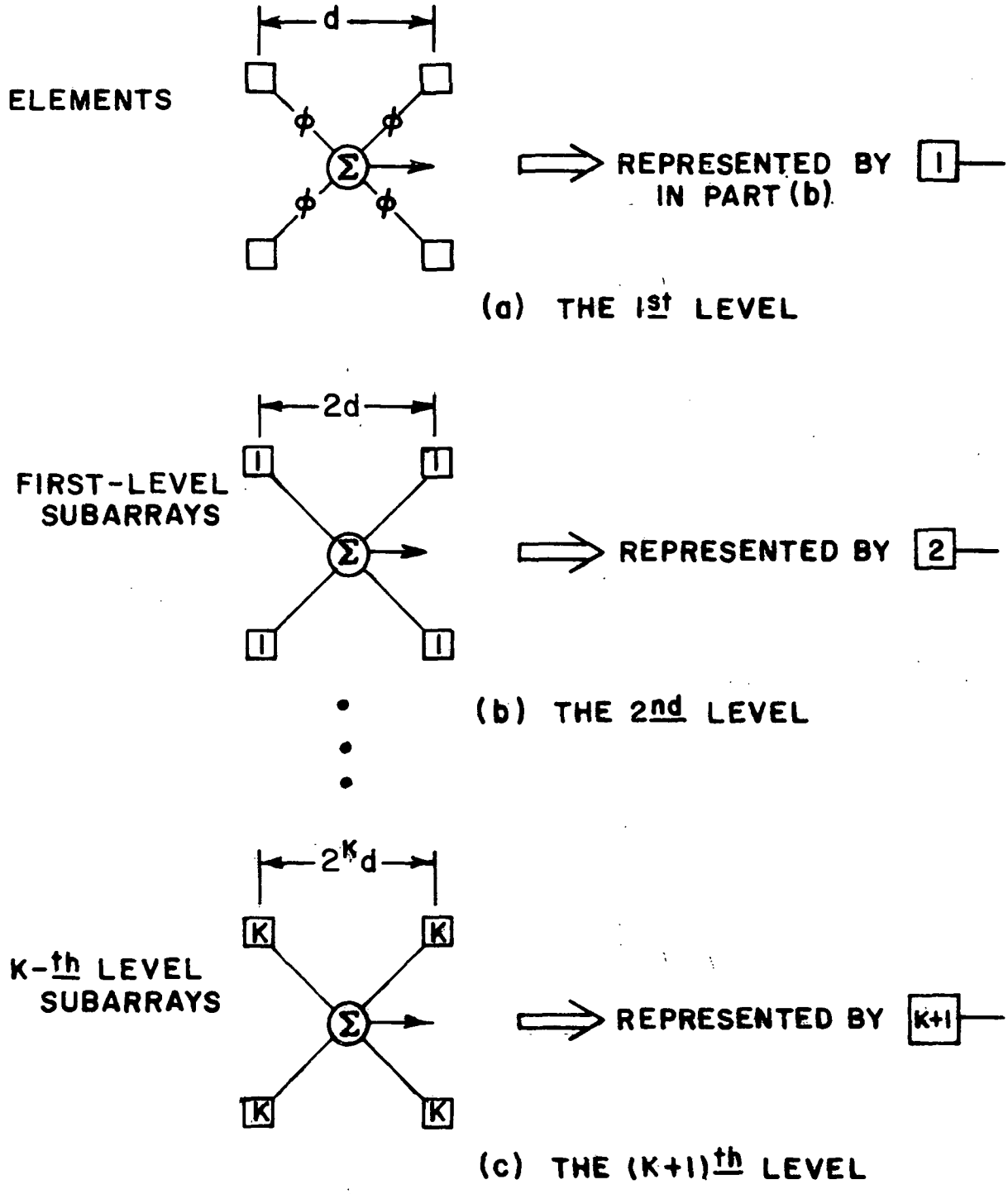

Figure 6. Recursive scheme for generation of two-dimensional corporate-fed array.

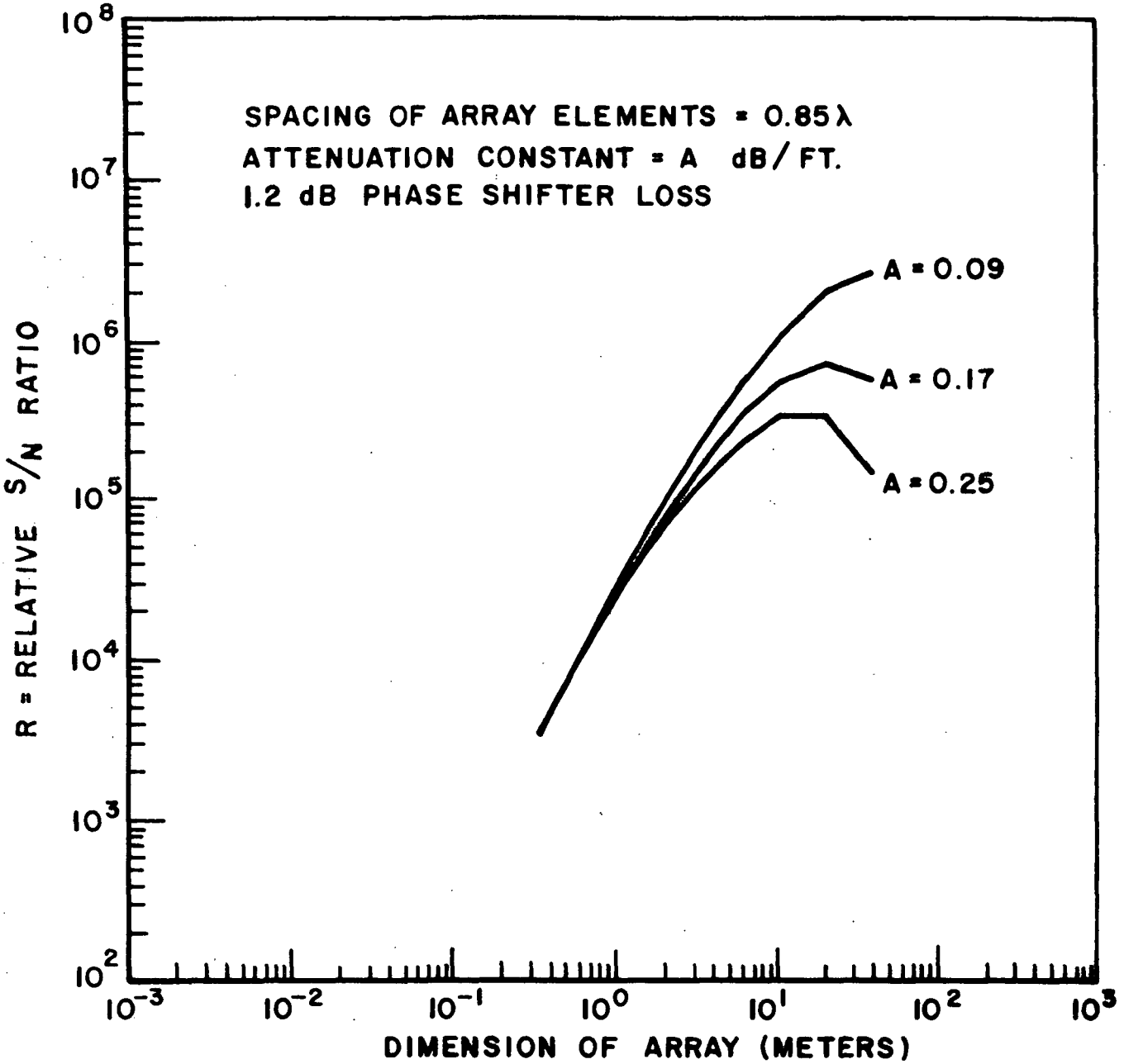

Figure 7. Normalized signal-to-noise ratio of the corporate array for reception of a single-directional signal at 30 GHz.

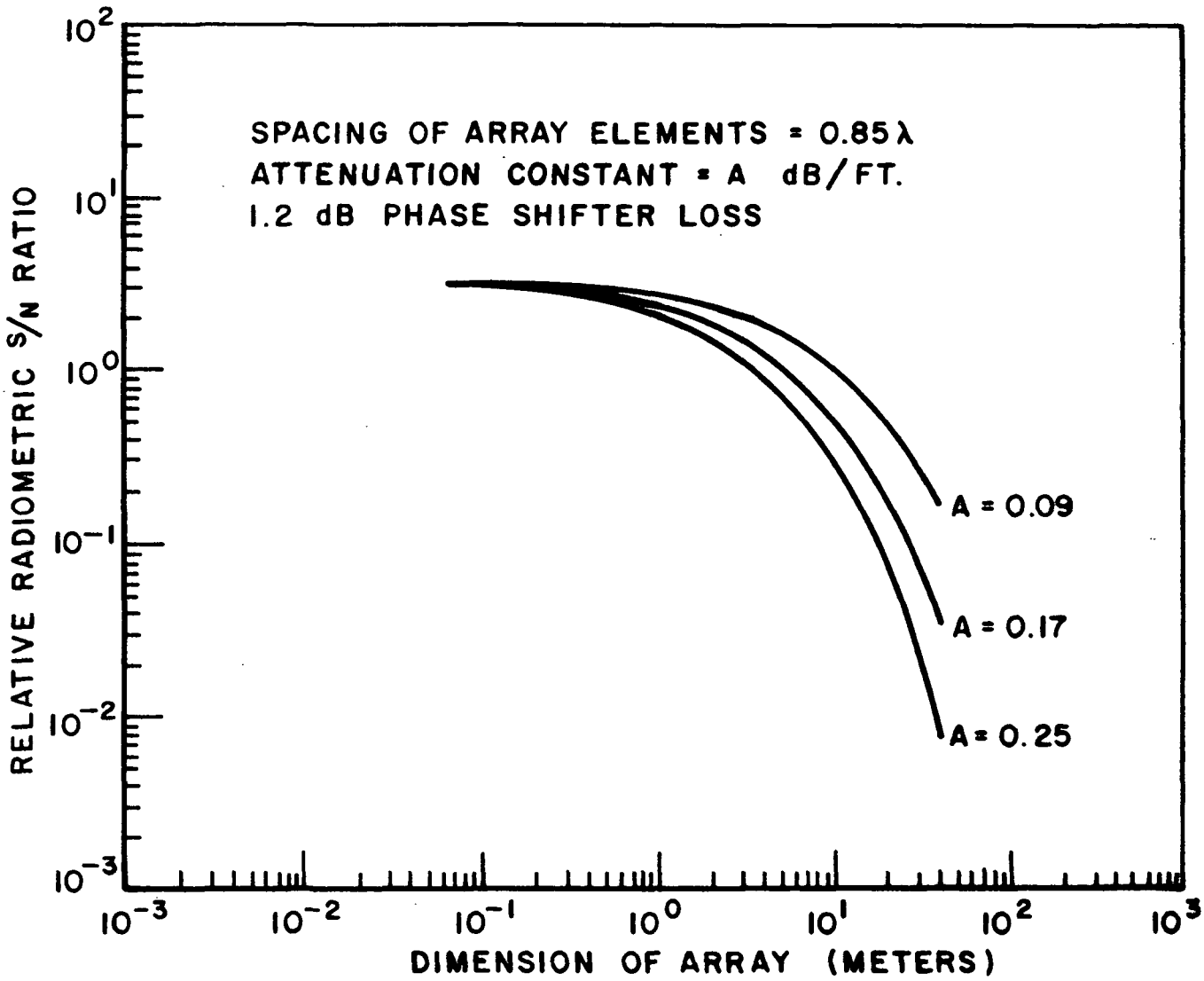

Figure 8. Relative signal-to-noise ratio of the corporate array for reception of a spatially uniform radiometric signal at 30 GHz.

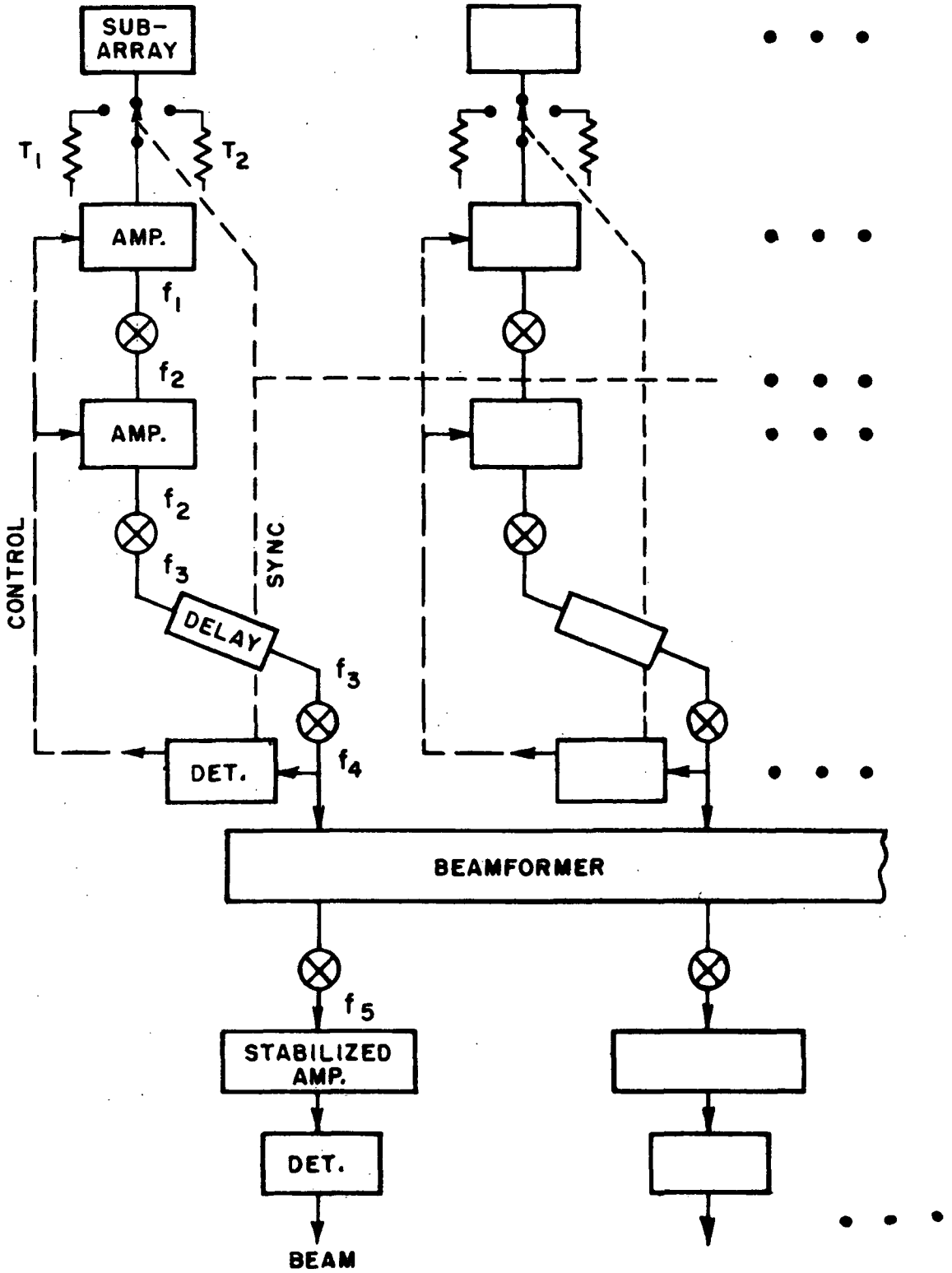

Figure 9. Modified Dicke receiver. The switches are distributed to allow the introduction of amplification at the subarray level. The preamplifiers may be inappropriate in some frequency ranges. The frequency conversions are chosen to facilitate designing of amplifiers, delay networks, and beamformer; not all indicated conversions may be necessary.

REFERENCES

1. AN/AAR-33 Airborne Radiometer System. Final Report. Sperry Rand Corporation, Clearwater, Florida, 1967. NTIS accession number AD 674 780.

2. W. E. Scull (director)" SEASAT-A Phase A Study Report, NASA Goddard Space Flight Center, Greenbelt, MD , pp. 3-120f, August 1973.

3. Final Report for the Electrically Scanning Microwave Radiometer for Nimbus E. Aerojet Electrosystems Co., Azusa, CA, January 1973. Company report 1740FR-1, NASA CR-132812, NTIS accession N73-32342.

4. Operations and Maintenance Manual Nimbus F Electrically Scanning Microwave Radiometer. Report 1741-OM-1, Contract NAS 5-21635. Aerojet Electrosystems Co., Azusa, CA, revised 1974.

5. Scientific Uses of the Space Shuttle. Space Science Board, National Research Council, National Academy of Sciences, Washington, D.C., 1974.

6. E. A. Wolff, Shuttle Communications Experiments. 1974. Document X-950-74-317, NASA Goddard Space Flight Center, Greenbelt, MD.

7. L. J. Ippolito, W.H. Kummer, C. A. Levis, "Space Shuttle Millimeter Wave Experiment." IEEE Intercon 75 paper E/3. 1975.

8. NASA Study, "Outlook for Space" as reported in Aviation Week and Space Technology, p. 39, March 8, 1976.

9. R. H. Dicke, "The Measurement of Thermal Radiation at Microwave Frequencies." Review of Scientific Instruments, v. 17, pp. 268-275. 1946.

10. M. E. Tiuri in Chapter 7 of Radio Astronomy by J. D. Kraus, McGraw-Hill, 1966.

11. H. C. Ko, Chapter 4 in Microwave Scanning Antennas, Vol. I., ed. by R. C. Hansen, Academic Press, 1964.

12. K. Fujimoto, "On the Correlation Radiometer Technique." IEEE Transactions on Microwave Theory and Techniques MTT-12, pp. 203-212, 1964.

13. H. C. Ko, op. cit., p. 277

14. A. E. Siegman, "Thermal Noise in Microwave Systems. Part 1, Fundamentals," Microwave Journal, v. 4, pp. 81-90, March 1961.

15. H. C. Lin, Noise Performance of Very Large Antenna Arrays. Report 3931-1, The ElectroScience Laboratory, Ohio State University, also available as NASA-CR-144716, NTIS accession no. N76-15333/7WY. 1975.

16. D. F. Wait, "Thermal Noise from a Passive Linear Multiport," IEEE Transactions MTT-16, pp. 687-691, Sept. 1968,

17. H. H. Grimm, "Noise Computations in Array Antenna Receiving Systems," Microwave Journal, v. 6, pp. 86-90, June 1963.

18. The VLA: A Proposal for a Very Large Array Radio Telescope, National Radio Astronomy Observatory, Green Bank, W. Va., 1967.

19. M. Ryle, "Radio Telescopes of Large Resolving Power," Reviews of Modern Physics, v. 47, pp. 557-566, July 1975.